Journal of Applied Fluid Mechanics, Vol. 12, No. 2, pp. 433-444, 2019.
Available online at www.jafmonline.net, ISSN 1735-3572, EISSN 1735-3645.
DOI: 10.29252/jafm.12.02.28867

Analytical Solution to the Boundary Layer Slip Flow and Heat Transfer over a Flat Plate using the Switching Differential Transform Method

H. H. Mehne[1†] and M. Esmaeili[2]

[1] *Aerospace Research Institute, Tehran, 14665-834, Iran*
[2] *Department of Mechanical Engineering, faculty of Engineering, Kharazmi University, Tehran, 15719-14911, Iran*

†*Corresponding Author Email:hmehne@ari.ac.ir*

(Received February 8, 2018; accepted August 14, 2018)

Abstract

In this paper, the two-dimensional steady boundary layer flow and heat transfer over a flat plate with slip velocity and temperature jump conditions at the walls were analyzed. Using similarity transforms, the governing equations were reduced to a system of ordinary differential equations. Semi-analytical solutions to the resulting boundary value problem were obtained using the differential transform method (DTM). In order to cover the asymptotic boundary conditions, a method of switching curves was proposed. In this switching approach, the traditional solution to the DTM, which is valid for finite horizons, was followed by another path that was also an analytical solution to the problem. The main preference of the resulting closed form solution with respect to numerical solution is the possibility of parametric studies. The method was verified using some available numerical data, and the results showed that our proposed method had reasonable efficiency and accuracy.

Keywords: Shape optimization; Optimization; Heat transfer; Approximation.

NOMENCLATURE

C_p	fluid heat capacity
f	transformed velocity
k	fluid thermal conductivity
Kn	Knudsen number
l	characteristic length
Pr	Prandtl number
Re	Reynolds number
T	temperature
T_g	gas temperature adjacent to the wall
T_w	wall temperature
T_∞	free-stream temperature
u	stream-wise velocity component
u_g	gas velocity adjacent to the wall
U_∞	free-stream velocity
u_w	wall velocity
ν	fluid kinematic viscosity
v	velocity component vertical to stream directions
x	component of the coordinate system
y	component of the coordinate system
σ_M	tangential momentum coefficient
α	non-dimensional velocity parameter
β	non-dimensional thermal slip parameter
γ	specific heat ratio
η	similarity variable
θ	transformed temperature
λ	free path
σ_T	thermal accommodation coefficient
ρ	fluid density
ψ	stream function

1. INTODUCTION

Boundary layer flow theory has been of interest to many researchers in fluid mechanics, and its various applications appear in many real world situations. Boundary layer theory was initially developed by some pioneering publications (Blasius 1907, Falkner and Skan 1931, Prandtl 1905, Sakiadis 1961), and comprehensive reviews of this theory and related topics are given by Caflisch and

Sammartino(2000), Garratt (1990), Kachanov (1994), Oleinik and Samokhin (1999), Schlichting *et al.* (1995), Tani (1977), and Weinan (2000). Among the different aspects of the theory, the problem of laminar boundary layers and heat transfer flow on a semi-infinite flat plate, called Blasius boundary layer flow, have been broadly studied (e.g. see Aziz 2009, Bataller 2008, Bhattacharyya 2011, Cortell 2008), where the latter can be used as abenchmark flow for the validation of different numerical methods (Cortell 2005 and Wang 2004).

During recent years, with the rapid development of micro-and nano-measuring science and technologies, it has been found that there are many significant differences between fluid flow at macroscopic scales and that at micro/nano scales, e.g. the wall-slip phenomena (Kumaranand Pop 2011). Rarefied gas flows with slip boundary conditions are often countered in micro-scale devices and low-pressure situations (Gad-el-Hak 1999). The effects of slip conditions are very important in technological applications for some fluids that exhibit wall slip, e.g. when polishing artificial heart valves and their internal cavities. The first reference that proposed boundary layer with slip condition is Beavers and Joseph (1967), where the effect of the boundary layer was replaced by the slip velocity. In the work of Martin and Boyd (2001), the slip flow condition was added to the Blasius problem in order to study microelectromechanical system (MEMS) scale flows. Among more recent studies (Aziz *et al.*2015, Aziz *et al.* 2014, Cai 2015 and Parida *et al.* 2015), Aziz *et al.*2015 considered the convective boundary layer flow of a power-law fluid on a porous plate with suction/injection. They investigated the effects of different physical parameters, such as the power-law index, slip, and permeability on the fluid flow and heat transfer characteristics.

In the present paper, the Blasius boundary layer and heat transfer flow with slip boundary conditions were studied. Applying the differential transform method (DTM) led to closed forms of the solutions to this problem. Introduced by Zhou (1986), the DTM was originally an analytical method for solving initial value problems. The method was subsequently extended and adopted to solve various mathematical problems such as boundary value problems, partial differential equations and integral equations (Usmanet *al.* 2017, Sepasgozar *et al.* 2017, Sheikholeslami and Ganji 2015, Mosayebidorcheh *et al.* 2017, Vimala and Omega 2016, Mosayebidorcheh 2015 and Thiagarajan and Senthilkumar 2013). A recent application of this method appears, for example, in Usman *et al.* (2017), where the DTM was applied to study the two unsteady phases of a nano fluid flow and heat transfer between moving parallel plates in the presence of a magnetic field. In the work of Sepasgozar *et al.* (2017), the analytical solutions of the momentum and heat transfer equations of a non-Newtonian fluid flowing in an axisymmetric channel with a porous wall were obtained via the DTM. This method was also used successfully by Sheikholeslami and Ganji (2015) to solve the problem of nano fluid hydro thermals in the presence of a variable magnetic field. A hybrid versionof the DTM and the finite difference method was also developed to solve flow and heat transfer equations by Mosayebidorcheh *et al.* (2017).

In the problems considered in the current paper, there are two boundary conditions at infinity. As the validity of the regular DTM is restricted to finite horizons, the related solution diverges over this range, and therefore the asymptotic behavior of the solution is not attained. The traditional method used to cover asymptotic conditions is to represent the polynomial solution with a rational function, i.e. a Padé approximation (Rashidi 2010). However, this approach and the consequent solutions depend on the degree of the polynomials used in the numerator and denominator. Therefore, determining the best fitting values of these parameters is based on trial and error. In the approach of this paper, the switching of the DTM result to a solution that satisfied the final boundary condition, and joint restriction, was introduced. In comparison with the Padé approximation, the proposed method was not based on trial and error, but instead it provided a systematic procedure to find the optimal location of switching. Therefore, the novelty of our method lies in introducing this technique. In order to check the validity and accuracy of the method, we applied it to different examples with and without the slip condition. Comparison of our results with those published in the literature confirmed the efficiency of our proposed approach.

2. MATHEMATICAL FORMULATION

The steady two-dimensional laminar viscous fluid flow and heat transfer over a flat plate were considered in this study. The governing equations for the conservation of mass, momentum and energy, based on the boundary layer approximation, can be expressed as:

$$\frac{\partial u}{\partial x}+\frac{\partial v}{\partial y}=0 \tag{1}$$

$$u\frac{\partial u}{\partial x}+v\frac{\partial u}{\partial y}=\nu\frac{\partial^2 u}{\partial y^2} \tag{2}$$

$$u\frac{\partial T}{\partial x}+v\frac{\partial T}{\partial y}=\frac{k}{\rho C_p}\frac{\partial^2 T}{\partial y^2} \tag{3}$$

where T is the temperature, u and v are the velocity components in the stream-wise and vertical directions, respectively, ν is the fluid's kinematic viscosity, k is the fluid's thermal conductivity, C_p is the fluid's heat capacity, and ρ is the fluid's density.

Considering the no-slip and constant temperature conditions on the wall, and the free-stream condition outside of the boundary layer, the proper boundary conditions of the boundary layer flow over a flat plat are given by:

$$u(x,0)=0, v(x,0)=0, T(x,0)=T_w \tag{4}$$

$$u(x,\infty)=U_\infty, v(x,\infty)=0, T(x,\infty)=T_\infty \tag{5}$$

Where T_w is the wall's temperature, and U_∞ and T_∞ are the free-stream's velocity and temperature, respectively. For flows with $Kn \le 0.001$, where $Kn=\lambda/l$ is the Knudsen number that is defined as the mean free path (λ) divided by the characteristic length (l), the no-slip and constant temperature conditions are valid. In the slip flow regime, $0.001 \le Kn \le 0.1$, and following slip boundary conditions can be used (Cai 2015):

$$u_g-u_w=\frac{2-\sigma_M}{\sigma_M}\lambda\left(\frac{\partial u}{\partial y}\right)_{y=0}+\frac{3\upsilon}{4T_g}\left(\frac{\partial T}{\partial x}\right)_w \tag{6}$$

$$T_g-T_w=\frac{2-\sigma_T}{\sigma_T}\frac{2\gamma}{\gamma+1}\frac{\lambda}{\Pr}\left(\frac{\partial T}{\partial y}\right)_{y=0} \tag{7}$$

where the w and g subscripts represent the wall and the adjacent gas, respectively. In addition, σ_M and σ_T are the tangential momentum and thermal accommodation coefficients, respectively, $\Pr$ is the Prandtl number, and γ is the specific heat ratio. The second term in Eq. (6) contains the stream-wise temperature gradient, also called the thermal creep, which is neglected in this study.

By introducing the following similarity transformations:

$$f(\eta)=\frac{\psi}{\sqrt{\upsilon x U_\infty}}, \theta(\eta)=\frac{T-T_\infty}{T_w-T_\infty} \tag{8}$$

$$\eta=y\sqrt{\frac{U_\infty}{\upsilon x}} \tag{9}$$

the variables are transformed from (x,y) to (x,η). Here η is a similarity variable and ψ is the stream function defined as:

$$u=\frac{\partial\psi}{\partial y}, \ v=-\frac{\partial\psi}{\partial x} \tag{10}$$

The velocity components also are based on the stream function as:

$$u=U_\infty f'(\eta), \ v=\frac{1}{2}(\eta f'-f)\sqrt{\frac{\upsilon U_\infty}{x}} \tag{11}$$

By substituting Eqs. (9) and (11) into the momentum and energy equations (Eqs. (2) and (3)), the following system of ordinary differential equations (ODE) is obtained:

$$2f'''+ff''=0, \tag{12}$$

$$2\theta''+\Pr f\theta'=0, \tag{13}$$

The boundary equations are also transformed into the following form as:

$$f(0)=0, f'(\infty)=1, f'(0)=\delta f''(0), \quad \delta=\frac{2-\sigma_M}{\sigma_M}Kn_x \operatorname{Re}_x^{1/2} \tag{14}$$

$$\theta(\infty)=0, \ \theta(0)=1+\beta\theta'(0), \quad \beta=\frac{2-\sigma_T}{\sigma_T}\frac{2\gamma}{\gamma+1}\frac{Kn_x}{\Pr}\operatorname{Re}_x^{1/2} \tag{15}$$

where Kn_x and Re_x are, respectively, the Knudsen and Reynolds numbers based on x, and δ and β are the non-dimensional velocity and thermal slip parameters, respectively.

Using the viscosity definition based on the kinetic theory of gases (Cai 2015 and Howarth 1938), we find:

$$\nu=\frac{\lambda}{3}\sqrt{\frac{8RT}{\pi}} \tag{15}$$

Based on the kinetic gas estimation of the viscosity, the slip boundary conditions can be also expressed as follows:

$$\frac{f'(0)}{f''(0)}=\delta=\frac{2-\sigma_M}{\sigma_M}\sqrt{\frac{3}{2}\sqrt{\frac{\gamma\pi}{2}}M_0}\left(\frac{x}{\lambda}\right)^{-1/2} \tag{16}$$

$$\frac{\theta(0)-1}{\theta'(0)}=\beta=\frac{2-\sigma_T}{\sigma_T}\frac{2\gamma}{\gamma+1}\frac{1}{\Pr}\sqrt{\frac{3}{2}\sqrt{\frac{\gamma\pi}{2}}M_0}\left(\frac{x}{\lambda}\right)^{-1/2} \tag{17}$$

3. METHOD OF SOLUTION

3.1 The Traditional DTM

Herein, we review some basic definitions of the differential transform, which were initially introduced by Zhou (1986):

Definition 1: If $y(t)$ is an analytical function in domain $T\subseteq\mathbb{R}$, then it can be differentiated continuously with respect to t. Let $t_0\in T$ be fixed, then the differential transform of this function at t_0 is defined as a sequence $\{Y(0), Y(1), Y(2), \ldots\}$, in which:

$$Y(k)=\left(\frac{d^k y}{dt^k}\right)_{t=t_0},k=0,1,2,... \tag{18}$$

It is clear that $Y(k)$, which is called the spectrum of $y(t)$, is the k-th coefficient in the Taylor series of $y(t)$ at $t=t_0$. Therefore, if D denotes the differential transform, then $y(t)$ is the inverse of the transform of $Y(k)$:

$$\begin{aligned} y(t)&=\sum_{k=0}^{\infty}\left(\frac{(t-t_0)^k}{k!}\right)Y(k) \\ &=D^{-1}\left(\{Y(0),Y(1),Y(2),\cdots\}\right) \end{aligned} \tag{19}$$

Some useful and important properties of the differential transforms are summarized in Table1. In this table, it is assumed that $R(k)$, $S(k)$, and $X(k)$ are the differential transforms of $r(t)$, $s(t)$, $x(t)$, respectively.

Table 1 Some properties of the differential transform

Original function	Transformed form
$x(t)=r(t)\pm s(t)$	$X(k)=R(k)\pm S(k)$
$x(t)=\alpha r(t)$, $\alpha\in\mathbb{R}$	$X(k)=\alpha R(k)$
$x(t)=r(t)s(t)$	$X(k)=\sum_{l=0}^{k}R(k)S(k-l)$
$x(t)=\frac{dr(t)}{dt}$	$X(k)=(k+1)R(k+1)$
$x(t)=\frac{d^n r(t)}{dt^n}$	$X(k)=\frac{(k+n)!}{k!}R(k+n)$
$x(t)=\int_{t_0}^{t}r(\tau)d\tau$	$X(k)=\frac{R(k-1)}{k},k\geq 1$
$x(t)=t^n$	$X(k)=\delta(k-n)=\begin{cases}1, & \text{if } k=n \\ 0, & \text{otherwise}\end{cases}$
$x(t)=e^{\lambda t}$	$X(k)=\frac{\lambda^k}{k!}$
$x(t)=\sin(\omega t+\alpha)$	$X(k)=\frac{\omega^k}{k!}\sin\left(\frac{k\pi}{2}+\alpha\right)$
$x(t)=\cos(\omega t+\alpha)$	$X(k)=\frac{\omega^k}{k!}\cos\left(\frac{k\pi}{2}+\alpha\right)$

When solving a two-point boundary equation with the DTM, the first step is to take the differential transform of both sides of the equation. If the original equation is:

$$L(y)=h(t) \tag{20}$$

Where $L(.)$ is thedifferential operator, then the equivalent equation in transformed form is:

$$D(L(y))=D(h(t)) \tag{21}$$

After performing the differential transform, this equation has an algebraic form like:

$$\mathcal{L}(Y(K))=\mathcal{H}(H(K)),\ k=0,1,2,\cdots \tag{22}$$

Where $Y(K)$ and $H(K)$ are the differential transforms of $y(.)$ and, $h(.)$ respectively. Equation (22) is also called the equivalent equation in the K-domain, which is usually a recursive iteration. If Eq. (22) is solved for $Y(K)$, then the solution of Eq. (20) will be calculated using Eq. (19).

When the initial conditions, for example when L is of the second degree, aregiven as:

$$y(t_0)=y_0,\ y'(t_0)=y'_0$$

Then the initial values for solving Eq. (22) are:

$$Y(0)=y_0, Y(1)=y'_0$$

When Eq. (20) has boundary conditions like:

$$y(t_0)=y_0,\ y(t_f)=y_f$$

Then the method starts with:

$$Y(0)=y_0,\ Y(1)=\alpha$$

Where α is a parameter that will be found by applying $y(t_f)=y_f$ at the end to the resulting solution of the form Eq. (19).

In the present problem of this paper, some finial conditions have an asymptotic form as:

$$f'(\infty)=1$$

Some references propose using the Padé approximation to approximate the resulting polynomial of Eq. (19) as a rational function, in order to find solutions that will have the appropriate asymptotic behavior.

3.2. The Switching DTM

In the proceeding section, we introduced a different approach based on switching to a second curve to satisfy the final conditions.

Lets take the differential transform from both sides of Eqs. (12)- (13). Then, the corresponding equations based on the properties inTable1 in *K*-space are:

$$F(k+3)=\frac{-1}{2(k+1)(k+2)(k+3)}\sum_{l=0}^{k}(l+1)(l+2)F(k-l)F(l+2),\quad k=1,2,\cdots \tag{23}$$

$$\Theta(k+2)=\frac{-\Pr}{2(k+1)(k+2)}\sum_{l=0}^{k}(l+1)F(k-l)\Theta(l+1),\quad k=1,2,\cdots \tag{24}$$

where $F(k)$ and $\Theta(k)$ denote the differential transforms of f and θ, respectively. To start the above iterations, the following initial conditions are employed, which are equivalent to the initial conditions of Eqs. (14) and (15), which are also in *K*-space:

$$F(0)=0,\ F(2)=\frac{1}{2\delta}F(1), \tag{25}$$

$$\Theta(0)=1+\beta\Theta(1), \tag{26}$$

With these initial conditions, the resulting coefficients obtained from Eqs. (23) and (24) are functions of $\Pr$, δ and β, that are given and two unknown coefficients $F(2)$ and $\Theta(1)$. These two coefficients are taken as parameters that control the final conditions of Eqs. (14) and (15) by defining:

$$f_2=F(2)=\frac{1}{2}f''(0), \tag{27}$$

$$t_1=\Theta(1)=\theta'(0), \tag{28}$$

Let us now consider that the resulting solutions to $f(.)$ and $\theta(.)$, which are infinite series, are truncated in N terms as follows:

$$f_N(\eta)=\sum_{k=0}^{N}F(k)\eta^k, \tag{29}$$

$$\theta_N(\eta)=\sum_{k=0}^{N}\Theta(k)\eta^k, \tag{30}$$

where $f_N(\eta)$ satisfies both Eq. (12) approximately, and its initial condition. In order to satisfy the final condition at infinity, we propose that the velocity profile is a constant value at a suitable point $\eta=\eta_\infty$ as follows:

$$f'(\eta)=\begin{cases} f_N'(\eta), & \eta\le\eta_\infty \\ 1, & \eta\ge\eta_\infty \end{cases} \tag{31}$$

Then, it satisfies the final condition $f'(\infty)=1$ trivially.

Now, η_∞ and f_2 are two parameters which have to be found in such a way that at the switch point, the value of the first derivative is 1 and the second derivatives must be as small as possible, that is $f'(\eta_\infty)=1$ and $f''(\eta_\infty)=0$. In order to find the optimal values of η_∞ and f_2, the following optimization problem needs to be solved numerically:

$$\min\left(\left(f'(\eta_\infty)-1\right)^2+\left(f''(\eta_\infty)\right)^2\right) \tag{32}$$

Similarly, the switched form of the temperature is assumed as:

$$\theta(\eta)=\begin{cases} \theta_N(\eta), & \eta\le\eta_\infty \\ \theta_\infty(\eta), & \eta\ge\eta_\infty \end{cases} \tag{33}$$

Unlike the final course curve for $f(\eta)$ in Eq. (31), which is a constant straight line, in the case of $\theta(\eta)$, some analytical effort is needed.

Due to the switching of $f'(\eta)$ at η_∞ to a constant value of 1, $f(\eta)$ has the form $a_0+\eta$ for $\eta>\eta_\infty$, where, $a_0=f_N(\eta_\infty)-\eta_\infty$ is a known constant. Therefore, Eq. (13) changes to the following format:

$$2\theta''+\Pr(a_0+\eta)\theta'=0, \tag{34}$$

or equivalently:

$$\frac{d(\theta')}{d\eta}=-\frac{1}{2}\Pr(a_0+\eta)\theta', \tag{35}$$

The above linear first-order equation can be solved for θ':

$$\frac{d(\theta')}{\theta'}=-\frac{1}{2}\Pr(a_0+\eta)d\eta \Rightarrow \mathrm{Ln}(\theta'(\eta))-\mathrm{Ln}(\theta'(\eta_\infty)) =-\frac{1}{2}\Pr\int_{\eta_\infty}^{\eta}(a_0+\xi)d\xi, \tag{36}$$

Therefore:

$$\theta'(\eta)=\theta'(\eta_\infty)\left[\exp\left(\frac{\Pr}{4}\left(f_N(\eta_\infty)\right)^2\right)\exp\left(-\frac{\Pr}{4}\left(f_N(\eta_\infty)-\eta_\infty+\eta\right)^2\right)\right] \tag{37}$$

By integrating the above equation, the final form of

$\theta(\eta)$ is found as:

$$\theta_\infty(\eta)=\theta(\eta_\infty)+\theta'(\eta_\infty)\exp\left(\frac{\Pr}{4}\left(f_N(\eta_\infty)\right)^2\right)\sqrt{\frac{\pi}{\Pr}}\left[\operatorname{Erf}\left(\frac{\sqrt{\Pr}}{2}\left(f_N(\eta_\infty)-\eta_\infty+\eta\right)\right)-\operatorname{Erf}\left(\frac{\sqrt{\Pr}}{2}\left(f_N(\eta_\infty)\right)\right)\right] \tag{38}$$

where $\operatorname{Erf}(x)$ is the error function defined as:

$$\operatorname{Erf}(x)=\frac{2}{\sqrt{\pi}}\int_0^x \exp\left(-s^2\right)ds \tag{39}$$

In order that the proposed solution to Eq. (33) is continuous, it should satisfied $\theta_N(\eta)=\theta_\infty(\eta)$ and $\theta'_N(\eta)=\theta'_\infty(\eta)\frac{1}{2}$ at $\eta=\eta_\infty$, which is established when $\theta_N(\eta_\infty)$ and $\theta'_N(\eta_\infty)$ are used in Eq. (39), that is:

$$\theta_\infty(\eta)=\theta_N(\eta_\infty)+\theta'_N(\eta_\infty)\exp\left(\frac{\Pr}{4}\left(f_N(\eta_\infty)\right)^2\right)\sqrt{\frac{\pi}{\Pr}}\left[\operatorname{Erf}\left(\frac{\sqrt{\Pr}}{2}\left(f_N(\eta_\infty)-\eta_\infty+\eta\right)\right)-\operatorname{Erf}\left(\frac{\sqrt{\Pr}}{2}\left(f_N(\eta_\infty)\right)\right)\right] \tag{40}$$

This solution should also satisfy the final condition $\theta(\infty)=0$. It is clear that the proposed solution has a parameter a_0, which we will use as a controlling parameter for its asymptote. Since the limit of the error function at infinity is 1, if we take the limit from $\theta_\infty(\eta)$ as $\eta\to+\infty$, we have:

$$\lim_{\eta\to+\infty}\theta_\infty(\eta)=\theta_N(\eta_\infty)+\theta'_N(\eta_\infty)\exp\left(\frac{\Pr}{4}\left(f_N(\eta_\infty)\right)^2\right)\sqrt{\frac{\pi}{\Pr}}\left[1-\operatorname{Erf}\left(\frac{\sqrt{\Pr}}{2}\left(f_N(\eta_\infty)\right)\right)\right] \tag{41}$$

Now, it is enough to solve the following equation for η_∞:

$$L(\eta_\infty,f_2,t_1)=-\theta_N(\eta_\infty)+\theta'_N(\eta_\infty)\exp\left(\frac{\Pr}{4}\left(f_N(\eta_\infty)\right)^2\right)\sqrt{\frac{\pi}{\Pr}}\left[1-\operatorname{Erf}\left(\frac{\sqrt{\Pr}}{2}\left(f_N(\eta_\infty)\right)\right)\right]=0 \tag{42}$$

But, as it has been seen before, η_∞ is estimated from Eq. (32), and in order to find its optimal value, Eq. (42) must be zero. Next, we can combine Eqs. (32) and (42) by minimizing the following objective function:

$$I(\eta_\infty,f_2,t_2)=\left(f'_N(\eta_\infty)-1\right)^2+\left(f''_N(\eta_\infty)\right)^2+\left(L(\eta_\infty,f_2,t_1)\right)^2 \tag{43}$$

By solving Eq. (43), the switch point of Eqs. (31) and (33), and the required parameters that satisfy the final conditions are obtained.

4. RESUTS

In this section, our proposed method was applied to three cases to demonstrate its accuracy and efficiency.

Case 1: In the simplest case, the following Blasius problem is considered, where the velocity slip δ is zero:

$$2f'''+ff''=0, \tag{44}$$
$$f(0)=0,\ f'(0)=0,\ f'(\infty)=1,$$

The corresponding equation in *K*-space is the following single recursive relation:

$$F(k+3)=\frac{-1}{2(k+1)(k+2)(k+3)}\sum_{l=0}^{k}(l+1)(l+2)F(k-l)F(l+2),\quad k=1,2,3,\cdots \tag{45}$$

The initial conditions are also translated as:

$$F(0)=0,\ F(1)=0, \tag{46}$$

It is also assumed that $f_2=F(2)=\frac{1}{2}f''(0)$ is a free parameter that will be obtained in such a way that the final condition $f'(\infty)=1$ is satisfied. In this example, the solution is expressed up to 17th power of η as follows:

$$f_{17}(\eta)=f_2\eta^2-\frac{f_2^{\,2}\eta^5}{60}+\frac{11f_2^{\,3}\eta^8}{20160}-\frac{5f_2^{\,4}\eta^{11}}{266112}+\frac{9299f_2^{\,5}\eta^{14}}{14529715200}-\frac{1272379f_2^{\,6}\eta^{17}}{59281238016000} \tag{47}$$

$$f_{17}'(\eta)=2f_2\eta-\frac{f_2^{\,2}\eta^4}{12}+\frac{11f_2^{\,3}\eta^7}{2520}-\frac{5f_2^{\,4}\eta^{10}}{24192}+\frac{9299f_2^{\,5}\eta^{13}}{1037836800}-\frac{1272379f_2^{\,6}\eta^{16}}{3487131648000}$$

$$f_{17}''(\eta)=2f_2-\frac{f_2^{\,2}\eta^3}{3}+\frac{11f_2^{\,3}\eta^6}{360}-\frac{25f_2^{\,4}\eta^9}{12096}+\frac{9299f_2^{\,5}\eta^{12}}{79833600}-\frac{1272379f_2^{\,6}\eta^{15}}{217945728000}$$

This solution gives a family of approximate solutions of the Blasius problem that satisfies the Blasius equation and initial conditions in a region of $\eta=0$. Now, the proposed solution that satisfies the final condition has a s witched form as:

$$f'(\eta)=\begin{cases} f_{17}'(\eta), & \eta\le\eta_\infty \\ 1, & \eta\ge\eta_\infty \end{cases} \tag{48}$$

Therefore, η_∞ and f_2 are two parameters which have to be found in such a way that at the switch point, the value of the first derivative is 1 and the second derivatives must be as small as possible, that is $f'(\eta_\infty)=1$ and $f''(\eta_\infty)=0$. In order to find the optimal values of η_∞ and f_2, the following optimization problem is solved numerically:

$$\min\left(\left(f'(\eta_\infty)-1\right)^2+\left(f''(\eta_\infty)\right)^2\right) \tag{49}$$

The optimal values of the decision variables are $\eta_\infty=3.96046$ and $f_2=0.180281$. The results are depicted in Figs. 1 and 2. In these figures, the computed results of $f(\eta)$ and its first and second derivatives are compared with the numerical results of Howarth (1938). As can be seen, very good agreement is observed between the results obtained with the switching DTM and the numerical results reported by Howarth (1938).

Another parameter that measures the quality of the solution is the absolute value of the difference of the two sides of the Blasius equation with the approximate solution put into the right hand side of Eq. (1). That is, $\text{Error}(f_N)=\left|2f_N'''+f_Nf_N''\right|$. A smaller $\text{Error}(f_N)$ means a better approximation. In Fig. 3, the corresponding errors are depicted for different number of terms.

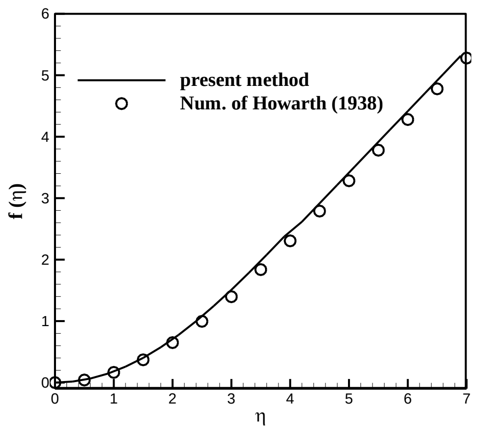

Fig. 1. The profile of $f(\eta)$ for case1. The solid line indicates presents our differential transform method (DTM) results, while the circles show the numerical results of Howarth (1938).

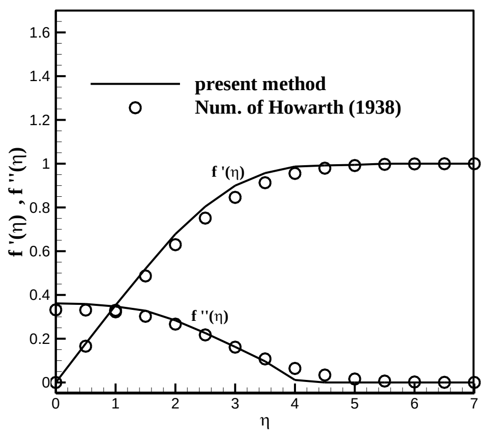

Fig. 2. The profiles of $f'(\eta)$ and $f''(\eta)$ for case1. The solid lines present our differential transform method (DTM) results, and the circles indicate the numerical results of Howarth (1938).

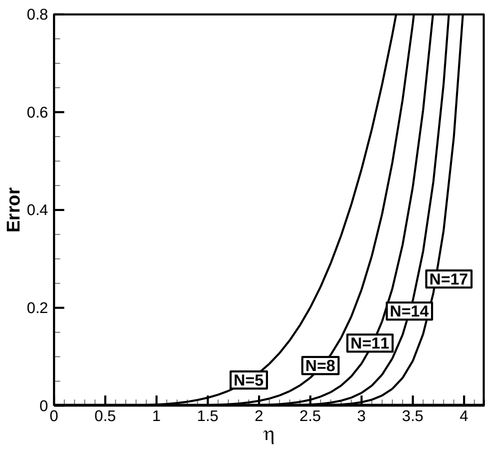

Fig. 3. Errors of the first part of the solution in case1.

It can be concluded from Fig. 3 that the validity of polynomial part of the solution changes with the order of the polynomial. The decreasing error from $N=5$ to $N=17$ shows that higher orders lead to better solutions of the differential equations. It is also noted that the error will increase after a near zero course, where the length of this favorable region increases with the polynomial's order. As the solution obtained with the proposed method has changed from a polynomial to a straight line at $\eta=\eta_\infty$, this grows of error lost its importance, while in the remaining, no errors are achieved. It should also be noted that in case 1 with $N=17$, the maximum error beyond $\eta=\eta_\infty$ is 0.65. Therefore, the solution obtained with our proposed method satisfies the Blasius equation with reasonable accuracy in its polynomial part, and when the error starts to increase, we switched to its straight line form, which is an exact solution to Eq. (1).

Case 2: In this case, the Blasius problem with $\delta\neq 0$ was considered. The boundary value problem is:

$$2f'''+ff''=0, \tag{50}$$

$$f(0)=0,\ f'(0)=\delta f''(0),\ f'(\infty)=1,$$

The corresponding equation in *K*-space is similar to thatof case1, but the second initial condition has changed to:

$$F(0)=0,\ F(2)=\frac{1}{2\delta}F(1), \tag{51}$$

So, with $f_1=F(1)$ as the unknown parameter, the general form of the semi-analytical solution up to the 8th power of η is found as:

$$\begin{aligned}f_8(\eta)&=f_1\eta+\frac{f_1\eta^2}{2\delta}-\frac{f_1^2\eta^4}{48\delta}-\frac{f_1^2\eta^5}{240\delta^2}\\&+\frac{f_1^3\eta^6}{960\delta}+\frac{11f_1^3\eta^7}{20160\delta^2}\\&+\frac{1}{672}\left(\frac{11f_1^3}{240\delta^3}-\frac{f_1^4}{32\delta}\right)\eta^8\end{aligned} \tag{52}$$

$$\begin{aligned}f_8'(\eta)&=f_1+\frac{f_1\eta}{\delta}-\frac{f_1^2\eta^3}{12\delta}-\frac{f_1^2\eta^4}{48\delta^2}+\frac{f_1^3\eta^5}{160\delta}\\&+\frac{11f_1^3\eta^6}{2880\delta^2}+\frac{1}{84}\left(\frac{11f_1^3}{240\delta^3}-\frac{f_1^4}{32\delta}\right)\eta^7\end{aligned}$$

$$\begin{aligned}f_8''(\eta)&=\frac{f_1}{\delta}-\frac{f_1^2\eta^2}{4\delta}-\frac{f_1^2\eta^3}{12\delta^2}+\frac{f_1^3\eta^4}{32\delta}\\&+\frac{11f_1^3\eta^5}{480\delta^2}+\frac{1}{12}\left(\frac{11f_1^3}{240\delta^3}-\frac{f_1^4}{32\delta}\right)\eta^6\end{aligned}$$

Computations for case 2 were performed for different values of δ. Figure 4 shows the normalized velocity profiles within the boundary layer for $\delta=0,1,2,3,4$ and 5. The velocity profile of $\delta=0$ represents the classical solution tothe Blasius flow in which the no-slip condition is imposed at the wall. As shown in Fig. 4, the normalized slip velocity $f'(0)$ increases with an increase in δ. As an example, for $\delta=2$, the values of $f'(\eta)$ are compared with the numerical result of Martin and Boyed (2001) obtained with the shooting method, where reasonable agreement is observed.

In Figs. 5 and 6 two important parameters, $f'(0)$ and $f''(0)$, which represent the normalized slip velocity and wall shear stress are shown, respectively. The accuracy of our results is confirmed by comparing them with the results of Martin and Boyed (2001). It is noted that when the Knudsen number is large enough, δ approaches infinity, and the normalized slip velocity and the wall shear stress approaches 1 and zero, respectively. This condition corresponds tocomplete slip flow (i.e. hundred percent slip at the wall).

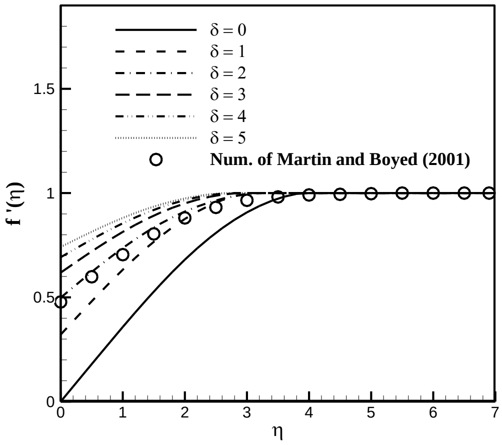

Fig. 4. Normalized velocity profiles ($\frac{u}{U_\infty}=f'(\eta)$) forcase2.The solid lines indicate our differential transform method (DTM) results for different values of δ, while the circles show the numerical results of Martin and Boyed (2001) for δ = 2 .

The percentage of friction reduction $\text{FR}=100\%\left(f''(0)\right]_{\delta=0}-f''(0))$ was also obtained for three different values of $\sigma_v=0.2, 0.5,$ and 0.8, as shown in Fig. 7. The results show that the friction is large at the initial portion of the plate, but then it reduces the rate proportional to the value of σ_v .

Case 3. In this case, boundary layer flow and heat transfer over a flat plate with velocity slip and thermal jump conditions are considered. So, the boundary value problem is expressed by Eqs. (12)-(15).

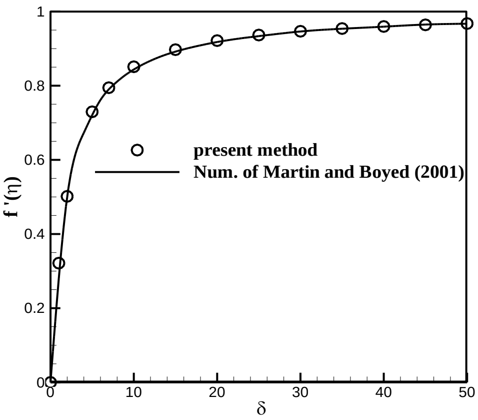

Fig. 5. Slip velocity ($\left.\frac{u}{U_\infty}\right]_{\text{wall}} = f'(0)$) for various values of δ for case2.The solid lines give ourdifferential transform method (DTM) results, and the circles indicate the numerical results of Martin and Boyed (2001).

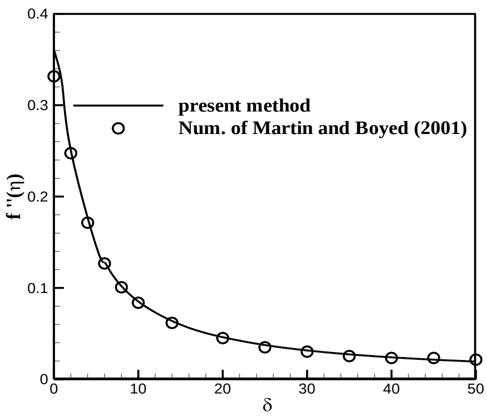

Fig. 6. Wall shear stress $\tau_w = \frac{\rho^{1/2}\mu^{1/2}U_\infty^{\ 1/2}}{x^{1/2}} f''(0)$ for various values of δ for case 2. The solid lines indicate thedifferential transform method (DTM) results, and the circles indicate the numerical results of Martin and Boyed (2001).

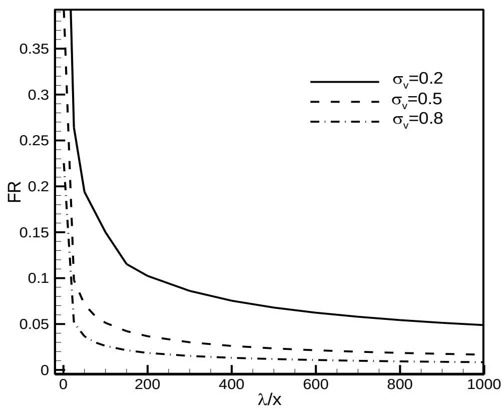

Fig. 7. The percentage of friction reduction in terms of x/λ for various values of σ_v for case2.

For example, with eight approximate terms, the solution has the following closed form:

$$\begin{aligned}\theta_8(\eta) &= 1+\beta t_1 + t_1\eta - \frac{1}{12} f_1 \Pr t_1 \eta^3 - \frac{f_1 \Pr t_1 \eta^4}{48\delta} \\ &+ \frac{1}{160} f_1^{\ 2} \Pr^2 t_1 \eta^5 \\ &- \frac{1}{60}\Pr\left(-\frac{f_1^{\ 2} t_1}{48\delta} - \frac{5 f_1^{\ 2}\Pr t_1}{24\delta}\right)\eta^6 \\ &- \frac{1}{84}\Pr\left(-\frac{f_1^{\ 2} t_1}{240\delta^2} - \frac{f_1^{\ 2}\Pr t_1}{24\delta^2} + \frac{1}{32} f_1^{\ 3}\Pr^2 t_1\right)\eta^7 \\ &- \frac{1}{112}\Pr\left[\frac{f_1^{\ 3} t_1}{960\delta} + \frac{f_1^{\ 3}\Pr t_1}{192\delta} + \frac{f_1^{\ 3}\Pr^2 t_1}{64\delta} \right. \\ &\left. - \frac{1}{10} f_1 \Pr\left(-\frac{f_1^{\ 2} t_1}{48\delta} - \frac{5 f_1^{\ 2}\Pr t_1}{24\delta}\right)\right]\eta^8\end{aligned} \tag{53}$$

$$\begin{aligned}\theta_8'(t) &= \eta - \frac{1}{4} f_1 \Pr t_1 \eta^2 - \frac{f_1 \Pr t_1 \eta^3}{12\delta} \\ &+ \frac{1}{32} f_1^{\ 2}\Pr^2 t_1 \eta^4 - \frac{1}{10}\Pr\left(-\frac{f_1^{\ 2} t_1}{48\delta} - \frac{5 f_1^{\ 2}\Pr t_1}{24\delta}\right)\eta^5 \\ &- \frac{1}{12}\Pr\left(-\frac{f_1^{\ 2} t_1}{240\delta^2} - \frac{f_1^{\ 2}\Pr t_1}{24\delta^2} + \frac{1}{32} f_1^{\ 3}\Pr^2 t_1\right)\eta^6 \\ &- \frac{1}{14}\Pr\left[\frac{f_1^{\ 3} t_1}{960\delta} + \frac{f_1^{\ 3}\Pr t_1}{192\delta} + \frac{f_1^{\ 3}\Pr^2 t_1}{64\delta} \right. \\ &\left. - \frac{1}{10} f_1 \Pr\left(-\frac{f_1^{\ 2} t_1}{48\delta} - \frac{5 f_1^{\ 2}\Pr t_1}{24\delta}\right)\right]\eta^7\end{aligned} \tag{54}$$

where $\Pr$, δ and β are given constants and f_1 and t_1 are parameters that control the solutions in order to match the final conditions. f_1, t_1 and η_∞ are found by minimizing Eq. (23).

As an example to check the accuracy of our method, we solved the problem for $\Pr = 0.5$, $\delta = 0.2$ and $\beta = 0.1$. The results for $N = 11$ are as follows:

$$\begin{aligned} f_{11}(\eta) &= 0.0753\eta + 0.1884\eta^2 \\ &- 0.0006\eta^4 - 0.0006\eta^5 \end{aligned} \tag{55}$$

$$\eta_\infty = 3.4284, \ f_1 = 0.0754$$

Due to rounding the coefficients to four decimal places, the confidences of η^6 to η^{11} are zero. Then, the complete solution is:

$$f(\eta) = \begin{cases} f_{11}(\eta), & \eta \le 3.4284 \\ 2.1849 + \eta, & \eta \ge 3.4284 \end{cases} \tag{56}$$

Moreover, when finding $\theta(\eta)$ the following results are obtained:

(57)

$$t_1 = -0.2433,\ a_0 = -3.2863$$

$$\theta_{11}(\eta) = 0.9756 - 0.2436\eta + 0.0008\eta^3 + 0.0009\eta^4$$

$$\theta_\infty(\eta) = 0.2722 - 0.2883\big(-0.0452 + \mathrm{Erf}\left[0.3535(-3.3151+\eta)\right]\big)$$

$$\theta(\eta) = \begin{cases} \theta_{11}(\eta), & \eta \le 3.4284 \\ \theta_\infty(\eta), & \eta \ge 3.4284 \end{cases}$$

In Figs. 8 and 9, the velocity and temperature profiles for case 3 are compared with the results of Bhattacharyya *et al.* (2011), respectively. Reasonable agreement between the switching DTM and the shooting method is clearly detected. The highest deviation of the normalized velocity from the numerical results of Bhattacharyya *et al.* (2011) is observed where the normalized velocity approaches 1 (i.e. close to the boundary layer's edge).

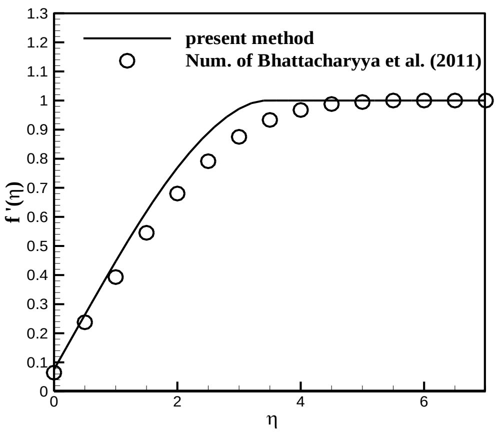

Fig. 8. The velocity profile of case 3 compared with the results of Bhattacharyya *et al.* (2011).

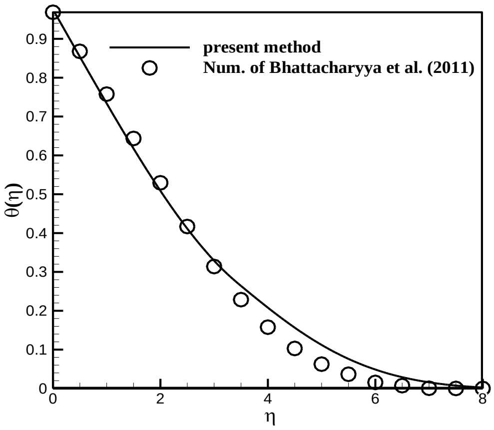

Fig. 9. The temperature profile forcase3 compared with the results of Bhattacharyya *et al.* (2011).

Moreover, to study the impact of thermal slip on heat transfer from the plate, the profiles of $\theta(\eta)$ and $\theta'(\eta)$ for values of $\beta = 0.0$, 0.3, 0.7, 1.3, and 2.0 are depicted in Figs. 10 and 11, respectively. These figures show that as the thermal slip increases, the magnitude of the temperature and its gradient monotonically decrease, which leads to weakening of the heat transfer from the plate.

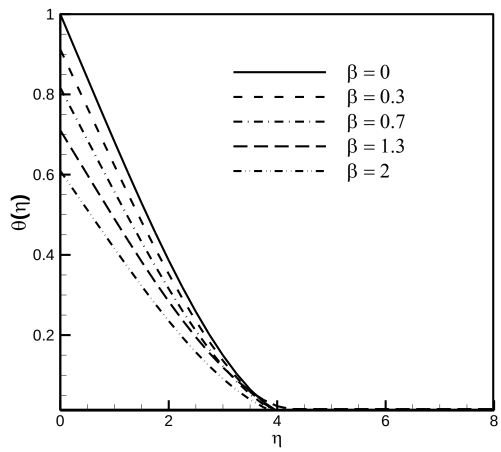

Fig. 10. Temperature profiles for case 3 against various values of the thermal slip.

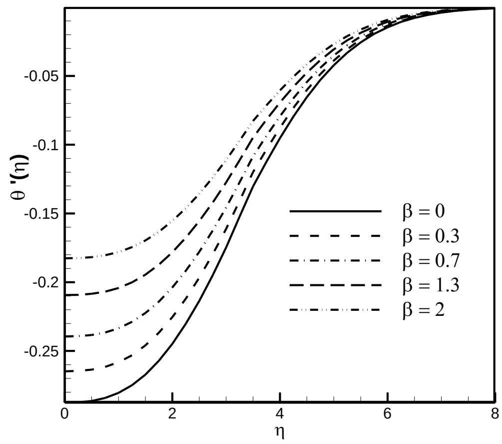

Fig. 11. Temperature gradient profiles for case 3 versus various values of the thermal slip.

The problem has been also solved for $\beta = 1.0$ and $\delta = 0.0$, 1.0, 3.0, and 8.0. In Fig. 12, the temperature profiles $\theta(\eta)$ of the various values of the velocity slip parameters are shown. As expected, the results indicate that when the slip parameter increases, the temperature reduces. Figure 13 demonstrates the temperature gradient profiles for the different velocity slip parameters. It is observed that, in an agreement with the results of Bhattacharyya *et al.* (2011), the temperature gradient decreases with δ before $\eta = 2$, and it increases after this point.

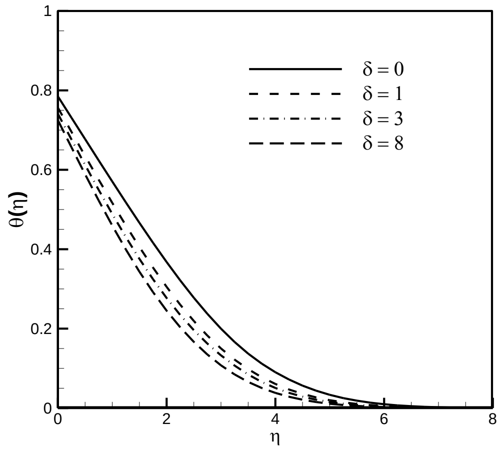

Fig. 12. Temperature profiles for case3 versus various values of the velocity slip.

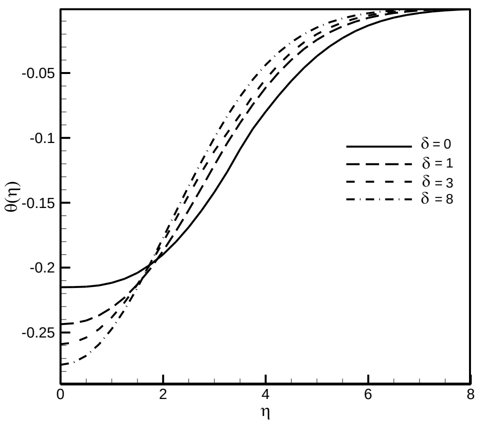

Fig. 13. Temperature gradient profiles for case 3 against various values of the velocity slip.

5. CONCLUSIONS

The switching DTM method was proposed in this paper to solve problems with asymptotic boundary conditions. The method was successfully applied to the boundary layer slip flow with heat transfer over a flat plate. The results revealed the accuracy of our method for different cases, which were comparable with other available numerical methods. The advantage of the proposed method with respect to numerical methods lies in the fact that with DTM, a semi-analytical solution will be obtained rather than a discrete one. The presented switching version of DTM did not contain the problem of choosing the degree of the numerator and denominator polynomials that appeared in the Padé approximation.

REFERENCES

Aziz, A. (2009). A similarity solution for laminar thermal boundary layer over a flat plate with a convective surface boundary condition. *Communications in Nonlinear Science and Numerical Simulation* 14(4), 1064-1068.

Aziz, A., J. I. Siddique and T. Aziz (2014). Steady boundary layer slip flow along with heat and mass transfer over a flat porous plate embedded in a porous medium. *PLoS ONE 9(12): e114544.*

Aziz, A., Y. Ali, T. Aziz and J. I. Siddique (2015). Heat Transfer Analysis for Stationary Boundary Layer Slip Flow of a Power-Law Fluid in a Darcy Porous Medium with Plate Suction/Injection. *PLoS ONE 10(9): e0138855.*

Bataller, R. C. (2008). Radiation effects for the Blasius and Sakiadis flows with a convective surface boundary condition. *Applied Mathematics and Computation* 206(2), 832-840.

Beavers, G. S. and D. D. Joseph (1967). Boundary conditions at a naturally permeable wall. *Journal of fluid mechanics* 30(1), 197-207.

Bhattacharyya, K., S. Mukhopadhyay and G. Layek (2011). MHD boundary layer slip flow and heat transfer over a flat plate. *Chinese Physics Letters* 28(2), 024701.

Blasius, H. (1907).*Grenzschichten in Flüssigkeiten mit kleiner Reibung*: Druck von BG Teubner.

Caflisch, R. and M. Sammartino (2000). Existence and singularities for the Prandtl boundary layer equations. *ZAMM-Journal of Applied Mathematics and Mechanics/Zeitschrift für Angewandte Mathematik und Mechanik* 80(11-12), 733-744.

Cai, C. (2015). Near continuum boundary layer flows at a flat plate. *Theoretical and Applied Mechanics Letters* 5(3), 134-139.

Cortell, R. (2005). Numerical solutions of the classical Blasius flat-plate problem. *Applied Mathematics and Computation* 170(1), 706-710.

Cortell, R. (2008). A numerical tackling on Sakiadis flow with thermal radiation. *Chinese Physics Letters* 25(4), 1340.

Falkner, V. and S. W. Skan (1931). Some approximate solutions of the boundary-layer equations. *The London, Edinburgh, and Dublin Philosophical Magazine and Journal of Science* 12, 865-896.

Gad-el-Hak, M. (1999). The fluid mechanics of microdevices-the Freeman scholar lecture. *Journal of Fluids Engineering* 121(1), 5-33.

Garratt, J. (1990). The internal boundary layer—a review. *Boundary-Layer Meteorology* 50(1-4), 171-203.

Howarth, L. (1938). On the solution of the laminar boundary layer equations. *Proceedings of the Royal Society of London A: Mathematical, Physical and EngineeringSciences* 164, 547-579.

Kachanov, Y. S. (1994). Physical mechanisms of laminar-boundary-layer transition. *Annual* *review of fluid mechanics* 26, 411-482.

Kumaran, V. and I. Pop (2011). Nearly parallel Blasius flow with slip. *Communications in Nonlinear Science and Numerical Simulation* 16, 4619-4624.

Martin, M. J. and I. D. Boyd (2001). Blasius boundary layer solution with slip flow conditions. *AIP Conference Proceedings*, 518-523.

Mosayebidorcheh, S., M. Hatami, D. Ganji, T. Mosayebidorcheh and S. Mirmohammadsadeghi (2015). Investigation of Transient MHD Couette flow and Heat Transfer of Dusty Fluid with Temperature-Dependent Oroperties. *Journal of Applied Fluid Mechanics* 8(4), 921-929.

Mosayebidorcheh, S., O. Makinde, D. Ganji and M. A. Chermahini (2017). DTM-FDM hybrid approach to unsteady MHD Couette flow and heat transfer of dusty fluid with variable properties. *Thermal Science and Engineering Progress* 2, 57-63.

Oleinik, O. A. and V. N. Samokhin (1999). *Mathematical models in boundary layer theory* 15: CRC Press.

Parida, S. K., S. Panda and B. Rout (2015). MHD boundary layer slip flow and radiative nonlinear heat transfer over a flat plate with variable fluid properties and thermophoresis. *Alexandria Engineering Journal* 54(4), 941-953.

Prandtl, L. (1905). Uber Flussigkeitsbewegung bei sehr kleiner Reibung. *Verhandl. 3rd Int. Math. Kongr. Heidelberg* (1904), Leipzig.

Rashidi. M. M., N. Laraqi and S. M. Sadri (2010). A novel analytical solution of mixed convection about an inclined flat plate embedded in a porous medium using the DTM-Padé. *International Journal of Thermal Sciences* 49(12), 2405-2412.

Sakiadis, B. (1961). Boundary-layer behavior on continuous solid surfaces: I. Boundary-layer equations for two-dimensional and axisymmetric flow. *AIChE Journal* 7, 26-28.

Schlichting, H., K. Gersten, E. Krause and H. Oertel (1995). *Boundary-layer theory* 7, Springer.

Sepasgozar, S., M. Faraji and P. Valipour (2017). Application of differential transformation method (DTM) for heat and mass transfer in a porous channel. *Propulsion and Power Research* 6(1), 41-48.

Sheikholeslami, M. and D. D. Ganji (2015). Nanofluid flow and heat transfer between parallel plates considering Brownian motion using DTM. *Computer Methods in Applied Mechanics and Engineering* 283(1), 651-663.

Tani, I. (1977). History of boundary layer theory. *Annual review of fluid mechanics* 9, 87-111.

Thiagarajan, M. and K. Senthilkumar (2013). DTM-Pade approximants for MHD flow with suction/blowing. *Journal of Applied Fluid Mechanics* 6(4), 537-543.

Usman, M., M. Hamid, U. Khan, S. T. M. Din, M. A. Iqbal and W. Wang (2017). Differential transform method for unsteady nanofluid flow and heat transfer. *Alexandria Engineering Journal*, in press.

Vimala, P. and P. B. Omega (2016). A Semi-Analytical Solution for a Porous Channel Flow of a Non-Newtonian Fluid. *Journal of Applied Fluid Mechanic* 9(6), 2707-2716.

Vincenti, W. G. and C. H. Kruger (1965). Introduction to physical gas dynamics. *Introduction to physical gas dynamics* New York, Wiley.

Wang, L. (2004). A new algorithm for solving classical Blasius equation. *Applied Mathematics and Computation* 157(1), 1-9.

Weinan, E. (2000). Boundary layer theory and the zero-viscosity limit of the Navier-Stokes equation. *Acta Mathematica Sinica* 16, 207-218.

Zhou, J. (1986). *Differential transformation and its applications for electrical circuits*, Huazhong University Press, Wuhan, China.